

# PCCP

Accepted Manuscript



This is an *Accepted Manuscript*, which has been through the Royal Society of Chemistry peer review process and has been accepted for publication.

*Accepted Manuscripts* are published online shortly after acceptance, before technical editing, formatting and proof reading. Using this free service, authors can make their results available to the community, in citable form, before we publish the edited article. We will replace this *Accepted Manuscript* with the edited and formatted *Advance Article* as soon as it is available.

You can find more information about *Accepted Manuscripts* in the [Information for Authors](#).

Please note that technical editing may introduce minor changes to the text and/or graphics, which may alter content. The journal's standard [Terms & Conditions](#) and the [Ethical guidelines](#) still apply. In no event shall the Royal Society of Chemistry be held responsible for any errors or omissions in this *Accepted Manuscript* or any consequences arising from the use of any information it contains.

**New insight into the formation mechanism of the Ag, Au  
and AgAu nanoparticles in aqueous alkaline media:  
alkoxides from alcohols, aldehydes and ketones as the  
universal reducing agent**

Janaina F. Gomes,<sup>\*</sup> Amanda C. Garcia, Eduardo B. Ferreira, Cleiton Pires,  
Vanessa L. Oliveira, Germano Tremiliosi-Filho and Luiz H. S. Gasparotto<sup>†</sup>

*Instituto de Química de São Carlos, Universidade de São Paulo,  
Caixa Postal 780, 13560-970, São Carlos, SP, Brazil*

---

<sup>\*</sup> *Current address: Departamento de Engenharia Química, Universidade Federal de São Carlos, 13565-905, São Carlos, SP, Brazil*

<sup>†</sup> *Current address: Instituto de Química, Universidade Federal do Rio Grande do Norte, Lagoa Nova, 59078-970, Natal, RN, Brazil*

*Corresponding authors: Dr. Janaina Fernandes Gomes (janainafg@ufscar.br)  
+55 16 3351-8921. Dr. Luiz H. S. Gasparotto (lhgasparotto@ufrnet.br)*

**Abstract**

In this report we present new insights into the formation mechanism of Ag, Au and AgAu nanoparticles with alcohols, aldehydes and ketones in alkaline medium at room temperature. We selected methanol, ethanol, glycerol, formaldehyde, acetaldehyde and acetone to demonstrate their capability of reducing gold and silver ions under the above-mentioned conditions. We showed that the particles are also formed with potassium tert-butoxide in the absence of hydroxides. Our results strongly suggest that alkoxides, formed from any molecule containing a hydroxyl or a functional group capable of generating it in alkaline medium, is the actual and universal reducing agent of silver and gold ions, in opposition to the currently accepted mechanisms. The universality of the reaction mechanism proposed in this work may impact on the production of noble nanoparticles with simple chemicals normally found in standard laboratories.

*Keywords: noble nanoparticles; alkaline media; alkoxide; electrocatalysis.*

## 1 – Introduction

Noble metal nanoparticles have found innumerable applications including photonics,<sup>1-2</sup> electrocatalysis,<sup>3-5</sup> chemical sensing,<sup>6</sup> biosensing<sup>7</sup> and catalysis.<sup>8-10</sup> Their synthesis usually involves the reduction of a precursor salt of the desired metal by sodium borohydride,<sup>11</sup> sodium citrate<sup>12</sup> and hydrazine.<sup>13</sup> Hydrazine is particularly efficient as reducing agent, however it should be avoided because it has many drawbacks such as carcinogenicity, environmental hazard and instability (specially in its anhydrous form).<sup>14</sup> Recently we reported an environmentally friendly route to produce gold<sup>15</sup> and silver<sup>16</sup> using glycerol as reducing agent in alkaline medium. Glycerol is a greener option since it is non-toxic and readily biodegradable under aerobic conditions. Sugar-persubstituted poly(amidoamine) dendrimers (sugar balls)<sup>17</sup> and glucose<sup>18</sup> have also been successfully applied as “green” reducers for the synthesis of gold and silver nanoparticles, respectively. Similarly to glycerol, both chemicals have a plenty of hydroxyl groups that are undoubtedly involved in the reaction. The question is how the hydroxyl groups participate in the reaction.

Herein we present new insights into the formation mechanism of gold (Au), silver (Ag) and gold-silver bimetallic (AuAg) nanoparticles (Nps). For the first time, we show evidences that the reducing agent is not the hydroxyl group itself, but the alkoxide formed from it in alkaline medium regardless of the identity of the starting molecule, provided that it contains hydroxyl groups or it is prone to generate them. Our results reveal that Au-Nps, Ag-Nps and AuAg-Nps

nanoparticles can be synthesized not only with glycerol, but also with methanol, ethanol, acetone, formaldehyde and acetaldehyde in alkaline medium at room temperature. Originally the reducing molecule must have either a hydroxyl or a carbonyl group that can form the hydroxyl through nucleophilic addition. In alkaline medium these hydroxyl groups are deprotonated to some extent. We argue here that the true reducing species is the corresponding alkoxide generated in high-pH media. Alkaline conditions are imperative since there was no formation of nanoparticles with glycerol, methanol, ethanol, acetone, formaldehyde and acetaldehyde in either neutral or acidic media. On the other hand, they were formed with potassium tert-butoxide in water (that is potassium ion + alkoxide) in the absence of hydroxides, supporting our discussion about the alkoxide as the main reducing species.

There are reports on synthesis of silver nanoparticles with ethylene glycol and glycerol<sup>19</sup> under alkaline conditions with NaOH being regarded as a mere accelerator. We show here that the OH<sup>-</sup> plays indeed a major role in the process. Formaldehyde in basic medium<sup>20</sup> has been previously employed for the silver nanoparticle production. In that work the authors proposed an implausible release (as explained later) of a hydride ion that would function as reducing species. It has been also shown that micrometric silver powder<sup>21</sup> can be obtained by reducing Ag<sup>+</sup> with acetone under alkaline medium. In the proposed mechanism a carbanion is formed by the abstraction of an  $\alpha$ -hydrogen. The carbanion subsequently reacts with either an acetone molecule or another carbanion releasing electrons for the reduction of Ag<sup>+</sup>. Herein it is proposed a

simple  $\text{OH}^-$  addition to the carbonyl group of the acetone, with subsequent formation of the alkoxide from the hydroxyl group in alkaline medium.

The results presented here represent a change of paradigm for the role of the hydroxyl groups on the formation of noble nanoparticles. The universality of the reaction mechanism proposed in this work may impact on the production of noble nanoparticles with simple chemicals normally found in standard laboratories, in contrast to the borohydride route, for example. The nanoparticles obtained with alkoxides as reducing agents are shown to be applicable for glycerol and borohydride electro-oxidations and oxygen electro-reduction. Due to the ease of production and scalability, their application may be expanded to other fields, such as to cancer therapy<sup>22</sup> and cancer cell imaging.<sup>23</sup>

## 2 – Experimental section

### 2.1 – Reagents and instrumentation

All chemicals (Aldrich) used in this work were of analytical grade and used without further purification. UV-vis spectra of the Au-Nps, Ag-NPs and AuAg-Nps colloidal suspensions were acquired with a Varian/Cary 5G spectrophotometer. For the TEM experiments, copper coated grids were immersed into the nanoparticle colloidal suspensions and allowed to dry overnight in a desiccator. The grids were then analyzed using either a TEM FEI Tecnai with an accelerating potential of 200 kV or a Magellan XRH scanning electron

microscope in the transmission mode with an accelerating potential of 30 kV. X-ray diffraction (XRD) measurements were carried out using a Rigaku diffractometer. Electrochemical experiments were conducted with an AUTOLAB 30 potentiostat/galvanostat controlled by the GPES software. High Performance Liquid Chromatography (HPLC) experiments were performed using a Shimadzu apparatus equipped with an ion-exclusion Aminex HPX-87H column, which separates the sample compounds by ascending pKa, and UV-vis ( $\lambda = 210$  nm) and refractometer detectors.

## 2.2 – Preparation of Au-Nps, Ag-Nps and AuAg-Nps

In a typical experiment for the production of colloidal monometallic nanoparticles, known amounts of polyvinylpyrrolidone (PVP) with molecular weight of 10.000, acting as stabilizing agent, with either  $\text{AuCl}_3$  (30% wt in HCl) or  $\text{AgNO}_3$  were dissolved in 5 mL of ultrapure water. In a separate flask, determined quantities of a reducer (one of the following: glycerol, methanol, ethanol, formaldehyde, acetaldehyde, acetone or potassium tert-butoxide) and NaOH were dissolved in 5 mL of ultrapure water. The reducer-NaOH solution was then added to the  $\text{AuCl}_3$ -PVP or  $\text{AgNO}_3$ -PVP solution to yield the following final concentrations:  $0.40 \text{ mmol L}^{-1} \text{ Au}^{3+}$ ,  $0.40 \text{ mmol L}^{-1} \text{ Ag}^+$ ,  $0.50 \text{ mol L}^{-1}$  reducer,  $0.010 \text{ mol L}^{-1} \text{ NaOH}$  and  $10 \text{ g L}^{-1}$  PVP. In the case of AuAg-Nps only results with glycerol will be reported. For the production of bimetallic nanoparticles 5 mL of a glycerol-NaOH solution was added to 5 mL of a solution containing both  $\text{Au}^{3+} +$

$\text{Ag}^+$  and PVP to yield the following final concentrations:  $0.20 \text{ mmol L}^{-1} \text{ Au}^{3+}$ ,  $0.20 \text{ mmol L}^{-1} \text{ Ag}^+$  and  $10 \text{ g L}^{-1} \text{ PVP}$ . The effect of pH on the shape of the bimetallic nanoparticles was evaluated by varying its value from 9 to 13, thus the amounts of NaOH were added accordingly. The colloidal suspensions were then characterized with UV-vis and TEM.

For the HPLC experiments, 1 mL of Ag and Au monometallic colloidal suspensions were prepared with  $0.010 \text{ mol L}^{-1} \text{ NaOH}$ ,  $0.010 \text{ mol L}^{-1} \text{ glycerol}$ ,  $0.40 \text{ mmol L}^{-1} \text{ AuCl}_3$  or  $0.40 \text{ mmol L}^{-1} \text{ AgCl}$ .

For the electrocatalytic experiments, the nanoparticles were produced directly onto Vulcan carbon without stabilization by PVP in order to avoid a potential influence of PVP on the reactions under study. The synthesis of the different catalysts consisted in sonicating 40 mg of XC-72 Vulcan carbon in 50 mL of ultrapure water and then adding a fixed amount of  $\text{AuCl}_3$  or  $\text{AgNO}_3$  (to produce monometallic NPs/C) and appropriate amount of a mixture containing  $\text{AuCl}_3 + \text{AgNO}_3$  (to produce bimetallic AuAg/C) under stirring to promote homogenization. Afterwards, another aqueous solution containing glycerol and NaOH was added to give the following concentrations:  $0.40 \text{ mmol L}^{-1} \text{ Au}^{3+}$  (in the case of Au nanoparticles),  $0.40 \text{ mmol L}^{-1} \text{ Ag}^+$  (in the case of Ag nanoparticles),  $1.0 \text{ mol L}^{-1} \text{ glycerol}$  and  $0.10 \text{ mol L}^{-1} \text{ NaOH}$ . For the bimetallic nanoparticles the  $\text{Au}^{3+}$  and  $\text{Ag}^+$  final concentrations were both  $0.20 \text{ mmol L}^{-1}$ . The black suspensions were kept during 30 min under stirring at room temperature and then washed, filtered and dried at  $80 \text{ }^\circ\text{C}$  for 12 h.



### 2.3 – HPLC measurements

The HPLC experiments were carried out in isocratic elution mode. 20  $\mu\text{L}$  of the nanoparticle solutions were injected into the chromatographic column operating at 27  $^{\circ}\text{C}$ . 3.3  $\text{mmol L}^{-1}$  sulphuric acid was used as eluent at a flow rate of 0.6  $\text{mL min}^{-1}$ . Different alkoxide oxidation products were identified by comparing the retention time of the analyzed samples with their respective references, namely glyoxylic acid, hydroxypyruvic acid, dihydroxyacetone, glyceraldehyde, mesoxalic acid, formic acid, glycolic acid, glyceric acid, tartronic acid and oxalic acid in NaOH solution.

### 2.4 - Electrochemical measurements

A three-electrode conventional cell was used for the electrochemical experiments. A catalytic layer deposited on a glassy-carbon rotating-disk (RDE), a platinum foil and an Hg/HgO in 0.10  $\text{mol L}^{-1}$  or 1.0  $\text{mol L}^{-1}$  NaOH were employed as working, counter and reference electrodes, respectively. A glassy carbon disk ( $\phi = 5 \text{ mm}$ , geometric area = 0.196  $\text{cm}^2$ ) was used as substrate to prepare active layers of the catalysts. For the preparation of the catalytic layer 2.0 mg of Au/C, Ag/C or AuAg/C powder was suspended in a mixture containing 1 mL of isopropyl alcohol and 20  $\mu\text{L}$  of a Nafion solution (5 wt % in low aliphatic alcohol, from DuPont). After ultrasonic homogenization, 20  $\mu\text{L}$  of this ink was

deposited onto the glassy carbon electrode and the solvent was then evaporated at room temperature. The Au/C catalyst was tested for borohydride oxidation in O<sub>2</sub>-free 1.0 mol L<sup>-1</sup> NaOH + 1.0 mmol L<sup>-1</sup> NaBH<sub>4</sub> solution. The behavior of the Ag/C for oxygen reduction was evaluated in O<sub>2</sub>-saturated 1.0 mol L<sup>-1</sup> NaOH solutions. Finally, glycerol electro-oxidation was performed with the Au/C and AuAg/C catalysts in O<sub>2</sub>-free 0.10 mol L<sup>-1</sup> glycerol + 1.0 mol L<sup>-1</sup> NaOH.

### 3 – Results and discussion

#### Chemical and physical characterizations of the colloidal nanoparticles obtained with different alkoxide precursors

Fig. 1 shows a collection of the UV-vis spectra of the colloidal Au-Nps prepared at room temperature (~25 °C) using glycerol, ethanol, acetone and acetaldehyde in alkaline medium as reducing agents. The colloidal Au-Nps spectra presented a maximum absorbance at around 520 nm regardless of the employed chemical species in alkaline medium, a value typical for quasispherical gold nanoparticles.<sup>24-25</sup> All reducing agents generated deep-red-colored solutions, reflecting the surface plasmon band (SPB) characteristic for gold in the nanometric regime. The *inset* of Fig. 1 shows representative photographs of the colloidal solutions in neutral (or acid) and alkaline conditions. The red color is observed only in alkaline medium, suggesting that a common species might be

responsible for the reduction. This is the first evidence for the capability of all employed reducing agents in generating Au-Nps. The symmetry of the bands implies a fair similarity in the shape of the nanoparticles and low degree of aggregation in the solution.<sup>26</sup>

Fig. 2 shows TEM images of Au-Nps produced with the different chemical species in alkaline medium. Most of nanoparticles were spherical in shape, thus corroborating the UV-vis results, and their average sizes ranged between 4.6 nm and 7.6 nm (Table 1). Similarly, the method also applies for Ag-Nps, as shown by the UV-vis spectra in Fig. 3. This time methanol was tested as primary alcohol representative. All mixtures turned yellow immediately after adding the different chemical species under alkaline conditions to the  $\text{Ag}^+$  + PVP solution, as shown by the photographs in the *inset* of Fig. 3. No nanoparticle formation was observed under neutral or acid conditions, with the solution remaining colorless. The colloidal Ag-Nps had a maximum absorbance at around 410 nm, a value which is attributed to the silver SPB.

Fig. 4 shows TEM images of Ag-Nps synthesized by the different chemical species in alkaline medium. The Ag-Nps are larger than Au-Nps and tend to agglomerate. Specifically their average sizes varied from 10.7 nm to 36.1 nm, as presented in Table 1. We must point out that the present work did not seek synthesis optimization (in order to obtain monodispersivity, for example). The goal is to elucidate a universal mechanism of producing gold, silver and bimetallic nanoparticles at room temperature with common reagents found in standard laboratories. Investigation of parameters such as temperature, nature

and concentration of the stabilizer, concentration of the precursor and pH lead to optimized synthesis, for example in terms of nanoparticle size and shape, as we have reported in a recent paper.<sup>27</sup>

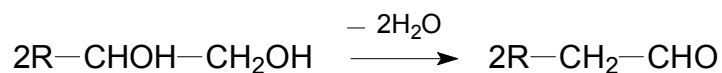
Fig. 5A presents absorption spectra of bimetallic AuAg-Nps acquired at  $\text{Au}^{3+}/\text{Ag}^+$  molar ratio of 0.5 with glycerol ( $0.10 \text{ mol L}^{-1}$ ) as reducing agent precursor at different pH values. Formation of bimetallic particles is evidenced by the presence of a single band whose  $\lambda_{\text{max}}$  strongly depended on the pH. A remarkable feature is the significant redshift of the surface plasmon band (SPB) maxima observed for pH 9 and 11 (554 nm and 543 nm, respectively) with respect to that for pure Au-Nps (520 nm, see Fig.1). According to previous studies,<sup>28-29</sup> the SPB maxima of AuAg-Nps were either located between those of pure Au and Ag nanoparticles (i.e. between 520 nm and 410 nm) or coincided with one of them. Moskovits et al.<sup>25</sup> demonstrated that these anomalous redshifts for samples with Au/Ag molar ratio of 0.5 are due to incomplete reduction of metal ions adsorbed on the surface of the nanoparticle and/or in the solution. This is probably true in our case because the availability of alkoxide, the species we will argue to be responsible for the reduction, increases with increasing pH at a fixed glycerol concentration. Considering a glycerol concentration of  $0.10 \text{ mol L}^{-1}$  and with its  $pK_a$  being 14.1, at pH of 9.0 and 13 the initial concentrations of the alkoxide are  $7.1 \times 10^{-7} \text{ mol L}^{-1}$  and  $7.1 \times 10^{-3} \text{ mol L}^{-1}$ , respectively. Note in Fig. 5A that the intensity of the absorption increases with pH, suggesting that the concentration of the reducing species is higher at strongly alkaline solutions. According to Chou et al.<sup>30</sup> it is possible that at the very

beginning of silver ion reduction some  $\text{Ag}_2\text{O}$  is formed, which later serves as nuclei for subsequent formation of Ag colloids. However, at pH 9, the amount of alkoxide would be far too low to reduce the  $\text{Ag}_2\text{O}$ , therefore  $\text{Au}^{3+}$  reduction would be prioritized with the formation of nanoparticles mainly constituted of gold. This is exactly what we discovered when EDS (Table 2) was performed on the nanoparticles shown in TEM images of Fig. 5B. Nanoparticles obtained at pH 9.0 and 11 are large and mainly constituted of gold, while those synthesized at pH 12 and 13 present smaller size and are silver enriched (also corroborated by the blueshift, Fig. 5A).

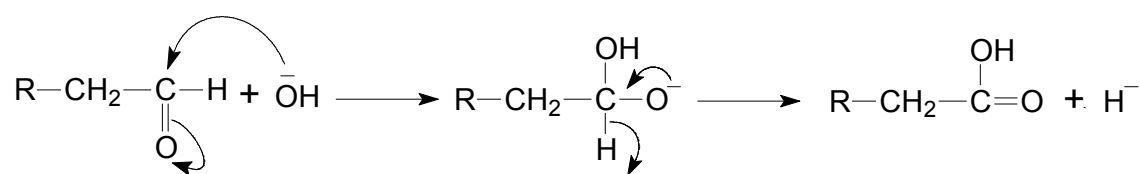
#### Formation mechanism of nanoparticles

The increased ability of some chemicals in reducing metallic ions under alkaline conditions has been explained thermodynamically.<sup>30</sup> In the presence of  $\text{OH}^-$  hydrazine and formaldehyde are stronger reducing agents because their standard potentials are more negative than in neutral conditions.<sup>33</sup> Although the thermodynamic argument is sufficient to explain the facilitated synthesis, it does not provide a mechanistic insight of the process. A mechanism for the polyol process was proposed by Fievet et al.<sup>34</sup> and supported by others.<sup>19, 35</sup> The polyol process consists in producing metallic powders through reduction of inorganic compounds in liquid polyols, such as ethylene glycol and glycerol. A generally accepted mechanism involves firstly alcohol dehydration to form an aldehyde<sup>19,</sup>

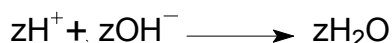
<sup>34</sup>.



the hydroxyl ion would then be added to the aldehyde through nucleophilic addition producing *hydride* ions and carboxylic acid (mostly in its ionized form due to the high pH)<sup>20</sup>:



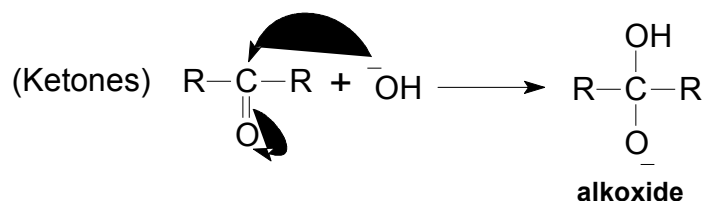
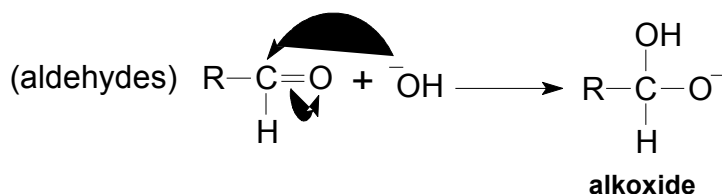
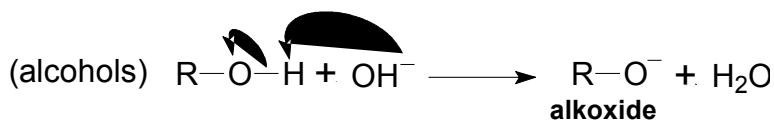
the hydride would then be responsible for the metal reduction and the proton released reacts with hydroxyl ions to generate water :



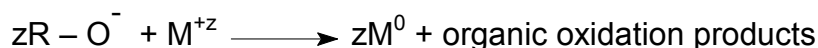
In our opinion the above mechanism is incorrect. Its major flaw is proposing the hydride as a leaving group for the nucleophilic addition. We propose that the reducing species is the alkoxide ion, the conjugate base of the alcohol formed due to the high pH. This species can be formed from alcohols as well as from aldehydes and ketones, explaining therefore the capability of all these chemicals to reduce gold and silver ions. The herein proposed mechanism is much more general as it accounts for the formation of nanoparticles from a single species, the alkoxide ion, regardless of its source.

The mechanism can be outlined as follows:

i) firstly, alkoxide is generated from alcohols, aldehydes or ketones, with the negative oxygen remaining deprotonated to some extent due to the high pH.



ii) the alkoxide then reduces the metal ion generating nanoparticles,



The identity of the organic oxidation products depends on the alkoxide precursor and also on the metallic ion to be reduced. In general primary alcohols can be oxidized to aldehydes and ultimately to carboxylic acids. In the next section we show that the oxidation products of glycerol/NaOH in the synthesis of Au-Nps may be oxalic acid, tartronic acid, hydroxypyruvic acid, glyceric acid and/or glyceraldehyde, dihydroxyacetone and formic acid, while the oxidation product of glycerol/NaOH in the synthesis of Ag-Nps is probably oxalic acid.

Carboxylate anions are not capable of generating nanoparticles at room temperature. We tried to conduct the synthesis of Au-Nps with sodium acetate as reducer without NaOH and no nanoparticle formation was observed. Only upon heating ( $\sim 80$  °C) the solution, it turned into a deep red characteristic of gold in the nanometric regime. The carboxylate anion is less prone to oxidation because it is stabilized by resonance. The negative charge is delocalized between the two oxygen atoms in a resonant structure. This may be the reason for the citrate-based synthesis to be carried out at relatively high temperatures ( $\sim 75$  °C -  $85$  °C).<sup>36</sup>

The mechanism proposed in this work is supported by the following reasons:

- 1) To confirm that the alkoxide is responsible for metal reduction we tested potassium tert-butoxide as reducing agent for the synthesis of gold and silver nanoparticles in the absence of NaOH. The solution containing gold and silver ions with PVP turned red and yellow, respectively, immediately after addition of tert-butoxide and the UV-vis spectra are shown in Fig. 6. Since the tert-butoxide anion is a pure alkoxide it must be the sole responsible for the reduction. Fig. 6 also shows TEM images of gold and silver nanoparticles produced by tert-butoxide without addition of NaOH, proving that tert-butoxide is indeed capable of generating Au and Ag nanoparticles. Regarding Ag-Nps, Selvakannan and co-workers<sup>37</sup> demonstrated the ability of the amino acid tyrosine to reduce  $\text{Ag}^+$  under



alkaline conditions. Tyrosine contains a phenol group that is ionized to phenolate ( $C_6H_5O^-$ , essentially an alkoxide) at high pH. This anion was then converted to quinone upon electron transfer to silver ions, as demonstrated by means of FTIR spectroscopy. Similarly to our studies, the authors observed that there was no formation of silver nanoparticles under neutral or acid pH conditions. This is further evidence that the alkoxide is responsible for the reduction.

- 2) The current accepted mechanism proposes that hydride ions play leaving-group roles in the nucleophilic-addition step. This is an unlikely postulate since good leaving groups must be weak conjugate bases.<sup>38</sup> The weaker the base, the better the leaving group. The  $pK_a$  of hydride is 42, which makes it an extremely strong base, thus a very poor leaving group. Therefore, hydride ions are not responsible for reducing metal ions because they cannot be generated in such conditions. Moreover, the reaction also works with acetone, a molecule that cannot release hydride anions but undergo nucleophilic addition to form the alkoxide. Another possibility with acetone, although possibly to a lesser extent, is the formation of the enolate anion due to the removal of an  $\alpha$ -hydrogen. The enolate is also an alkoxide and might play a role in reducing metal ions.
- 3) Another feature of the current accepted mechanism is the dehydration of alcohols to form aldehydes. Methanol, instead, does not undergo

dehydration reactions but was found to be capable of generating silver and gold nanoparticles in alkaline medium, as shown in Fig. 4 and in the UV-vis of gold nanoparticles SI 1 (supporting information), respectively. Given the slight acidity of methanol ( $pK_a = 15.5$ ), methoxide anions can be formed in alkaline medium and drive the nanoparticle formation.

- 4) Nanoparticles are also formed with PVP alone and dihydroxyacetone in alkaline medium at room temperature as shown in the UV-vis spectra of SI 2. PVP contains a ketone-carbonyl group that can undergo nucleophilic addition and then reduce gold ions. In this case PVP functions concomitantly as reducing and stabilizing agents. Dihydroxyacetone contains both hydroxyl and ketone groups to accomplish metal ion reduction. More importantly, none of these chemicals can release hydride, which makes the herein proposed mechanism more plausible.
- 5) The intensity of the UV-vis spectra in Fig. 5A was found to increase with increasing pH. This can be explained by the fact that the concentration of the alkoxide from glycerol also increased, thus generating a higher concentration of nanoparticles.

The mechanism proposed in this work is more general because it comprises a large variety of chemicals and is more plausible because it does not invoke hydride release.

*Analysis of alkoxide oxidation products formed during the synthesis of nanoparticles: HPLC results*

In this section we analyze the oxidation products of glycerol in NaOH formed during the synthesis of gold and silver nanoparticles.

Fig. 7 presents HPLC results collected at 1 min, 30 min and 60 min after mixing alkaline glycerol solution and the silver precursor salt solution. For comparison the chromatogram corresponding to glycerol in NaOH is also shown at the bottom of Fig. 7. A peak close to 6.5 min is observed already at 1 min of reaction and its intensity remains constant even after 60 min of reaction. No other peak emerges as function of the time. These results indicate that in the synthesis of the Ag-Nps silver ions are reduced at the expense of the alkoxide oxidation, which lead to the selective formation of only one detectable product. By comparing the retention time of the peak presented in Fig. 7 with those of reference samples (SI 3 in the supporting information), the oxidation product is probably oxalic acid in NaOH. Additionally, these results also reveal that the formation of Ag-Nps is completed below 1 min, in agreement with UV-vis results previously reported by our group.<sup>31</sup> We have shown that the formation of Ag-Nps passes through an induction period that corresponds to the first 15 s of reaction, followed by an exponential increase in the reaction velocity.<sup>31</sup>

Besides the alkoxide oxidation for the reduction of silver ions, we suspected that glycerol/NaOH could also be oxidized over the surface of the freshly prepared Ag-Nps in the reaction flask, although glycerol was previously

shown to be poorly oxidized over Ag-Nps in alkaline media between 0.05 V and 1.7 V vs. reversible hydrogen electrode.<sup>32</sup>

In order to investigate a possible oxidation of glycerol/NaOH over Ag-Nps, we prepared a suspension containing 3.6 mg of 10% wt. Ag/C (i.e. 0.36 mg Ag) and 1 mL of 0.010 mol L<sup>-1</sup> glycerol in 0.010 mol L<sup>-1</sup> NaOH. We used carbon-supported Ag-Nps here due to the difficulty of precipitating the Ag-Nps in the colloidal solution. The mass of silver used for the suspension preparation is around ten times higher than that of silver produced by the colloidal nanoparticles synthesis, while the volume of the glycerol/NaOH/Ag/C suspension is equivalent to that of the solution used in the nanoparticles synthesis. The ratio between the mass of Ag-Nps and the volume of glycerol/NaOH solution was multiplied by a factor of ca. 10 here in order to maximize the amount of possible reaction products from glycerol oxidation over Ag-Nps in alkaline medium. We evaluated then the chromatograms taken at 1 min, 30 min and 60 min after exposing the Ag/C to the glycerol/NaOH solution (SI 4). Two peaks between 6.0 min and 6.5 min of same magnitude orders are evidenced in the chromatograms of glycerol/NaOH in contact with Ag/C. The retention time of the peak closer to 6.0 min coincides with that of the peak related to the mobile phase, as seen by the chromatogram of glycerol in NaOH (at the bottom of SI 4). The peak closer to 6.5 min is possibly related to the formation of oxalic acid from glycerol/NaOH oxidation over the Ag/C. The ratio between the intensity of the peak related to the mobile phase and that of the oxalic acid peak increases with increasing exposition time, indicating that oxalic acid is gradually formed.

These results clearly demonstrate that glycerol in NaOH acts as reducing agent in the synthesis of Ag-Nps and additionally to that it may also be oxidized on the surface of the freshly prepared particles. Both reactions lead to the formation of oxalic acid, although the kinetic of glycerol/NaOH oxidation over Ag-Nps is very slow compared with that of the alkoxide oxidation for the silver ions reduction.

For the synthesis of the Au-Nps, HPLC results collected at 1 min, 30 min and 60 min after mixing glycerol/NaOH solution and the gold precursor salt solution are shown in Fig. 8. Different peaks between 6.0 min and 14 min are evidenced in the chromatograms and generally their intensity increases with increased reaction time, with exception of the peak closer to 6.0 min, whose intensity remains constant at 1 min, 30 min and 60 min. This peak is likely to be related with the mobile phase, while the other peaks are possibly associated with the formation of oxalic acid, tartronic acid, hydroxypyruvic acid, glyceric acid and/or glyceraldehyde, glycolic acid, dihydroxyacetone and formic acid, which are gradually formed from 1 min to 60 min of reaction time. These results suggest that in the synthesis of the Au-Nps gold ions are reduced as the alkoxide is oxidized.

As for Ag-Nps, we also investigated a possible oxidation of glycerol/NaOH over Au-Nps by HPLC. For these experiments, we prepared a suspension containing 4.0 mg of 30% wt. Ag/C (i.e. 1.20 mg Au) and 1 mL of 0.010 mol L<sup>-1</sup> glycerol in 0.010 mol L<sup>-1</sup>. The mass of gold used here is about thirty times higher than the mass of gold resulting from the nanoparticles synthesis method

described in the experimental section, whereas the volume of the suspension prepared here is equivalent to that of the solution used in the nanoparticles synthesis. In this way the formation of possible reaction products could be increased with respect to that from the glycerol oxidation on freshly prepared Au-Nps in the synthesis process. In SI 5 the chromatogram taken at 60 min after exposing the Au particles to the glycerol/NaOH solution is compared with that taken at 60 min after mixing glycerol/NaOH solution and the gold precursor salt solution during the Au-Nps synthesis. Some peaks are clearly evidenced in the chromatogram of glycerol/NaOH in contact with Au/C nanoparticles. However, their intensities are lower than those of the peaks seen in the chromatogram related to the Au-Nps synthesis. Therefore these results show that during the synthesis of Au-Nps the alkoxide from glycerol in NaOH reduces the gold ions to metallic particles and furthermore it can be oxidized on the surface of the freshly prepared Au-Nps, although the kinetic of glycerol/NaOH oxidation over Au-Nps is sluggish in comparison with that of the alkoxide oxidation for the gold ions reduction.

Summarizing, the HPLC results presented in this section attest for the capability of the alkoxide as reducing agent of the silver and gold ions.

#### *Electrocatalytic studies with Au-Nps, Ag-Nps and AuAg-Nps*

Au-Nps, Ag-Nps and AuAg-Nps were tested as catalysts for reactions of technological interest. Au-Nps were used to conduct the electro-oxidations of

borohydride (BOR) and glycerol, AuAg-Nps for glycerol electro-oxidation and Ag-Nps for oxygen electroreduction (ORR). The nanoparticles were synthesized directly onto carbon using glycerol as reducing agent without PVP stabilization in order to exclude any interference of PVP on the reactions under study. This implicated, on the other hand, in an increase of particle size due to lack of stabilization. With the help of the Scherrer equation<sup>39</sup> the mean crystallite size estimated for the Au/C, Ag/C and AuAg/C catalysts resulted in 22 nm, 15 nm and 13 nm, respectively, with data collected from XRD (SI 6). As expected, removal of PVP led to loss of control over the nanoparticle size. TEM images (Fig. 9A) revealed gold, silver and gold-silver nanoparticles of 6 nm to 20 nm, 5 nm to 15 nm and 5 nm to 25 nm in size, respectively. EDS analyses gave 10% wt of Au, Ag, and AuAg onto carbon.

Fig. 9B presents the electro-oxidation of glycerol and borohydride on Au/C, glycerol electro-oxidation on AuAg/C and the electroreduction of oxygen on Ag/C.

The blue curve is related to the RDE voltammogram at 1600 rpm in deaerated  $1.0 \text{ mol L}^{-1} \text{ NaOH} + 1.0 \text{ mmol L}^{-1} \text{ NaBH}_4$  on Au/C. The onset for  $\text{BH}_4^-$  oxidation is about  $-0.65 \text{ V}$ , implying an overpotential of  $0.69 \text{ V}$  since the theoretical oxidation potential of  $\text{BH}_4^-$  is  $-1.34 \text{ V}$  vs. Hg-HgO. Mass-transport limited current region is evident from  $-0.4 \text{ V}$  to  $0.3 \text{ V}$ . In a previous work<sup>15</sup> we showed that the number of electrons involved in the BOR at Au/C was 7.2, which is in good agreement with literature.

The red curve of Fig. 9B depicts a positive-going sweep for Au/C in O<sub>2</sub>-free 0.1 mol L<sup>-1</sup> glycerol + 0.10 mol L<sup>-1</sup> NaOH solution at 50 mV s<sup>-1</sup>. The onset for glycerol oxidation is about 0.05 V vs. Hg-HgO and a peak is developed at around 0.2 V vs. Hg-HgO. The current density then falls at higher potentials as a consequence of oxide formation, which inactivates the gold surface. Nevertheless, compared to platinum electrodes, gold is a more interesting catalyst than platinum for alcohols electro-oxidation in alkaline media at high potentials because it is more resistant towards surface oxide formation.<sup>40-41</sup>

The green curve is the positive-going polarization curve of glycerol electro-oxidation on AuAg/C in alkaline medium. When compared with Au/C, the AuAg/C material displayed lower current for glycerol electro-oxidation, therefore the current density has been magnified 10 times in order for it to be visible in the scale of the figure. Lower current means that the glycerol oxidation rate is smaller than the observed for Au/C. On the other hand, lower oxidation potential can be associated to a superior performance in terms of energy costs for the glycerol oxidation, with a decrease of about 120 mV in the onset potential, revealing a synergistic effect between gold and silver for this particular reaction. Finally, we applied the Ag/C material for the reduction of oxygen in alkaline conditions. Although microcrystalline Ag is considered a poor catalyst for the ORR, in the nanometric regime the activity is significantly improved due to the low area-to-volume ratio. In this context, Ag-Nps are good candidates as catalysts for oxygen cathodes in alkaline solutions.



The black curve of Fig. 9B presents a negative-going polarization curve of ORR for the Ag/C catalyst recorded in oxygen-saturated 1.0 M NaOH at 1600 rpm. The sharp peak at 0.22 V vs. Hg-HgO is due to the reduction of silver oxides formed at the beginning of the sweep. At about -0.1 V vs. Hg-HgO ORR sets in followed by the development of a diffusion-limited current density plateau between -0.4 V and -0.7 V. Theoretically the limiting-diffusion current value for an electrocatalyst that follows a 4-electron mechanism is  $3.28 \text{ mA cm}^{-2}$  at 1600 rpm in alkaline medium. For Ag/C in 1.0 M NaOH, the determined value was  $2.3 \text{ mA cm}^{-2}$ . As previously demonstrated<sup>16</sup> the discrepancy between the observed and theoretical values lies on the fact that the carbon support also contributes for ORR, however with only two electrons, therefore decreasing the overall efficiency.

We should emphasize that the activity towards ORR, BOR and glycerol oxidation can be enhanced by decreasing the particle size through optimization of the synthesis, an aspect we did not seek in this paper. Herein we aimed in showing the potentiality of an inexpensive and environmentally friendly method to produce active nanoparticles with alkoxides from alcohols, aldehydes and ketones in alkaline medium at room temperature.

#### 4 – Conclusions

We presented new insights into the formation mechanism of gold, silver and gold-silver bimetallic nanoparticles with alcohols, aldehydes and ketones in

alkaline medium. Alkalinity was found to be preponderant for nanoparticles formation. We showed that the reducer precursor must have a hydroxyl group or have the potentiality of generating it in alkaline medium. We propose that the reducing species of gold and silver ions is in fact the alkoxide, in opposition to the currently accepted mechanisms.

### Acknowledgements

The authors thank CNPq (Grant n° 471794/2012-0) and FAPESP for the overall support of this research.

### References

1. Kazeminezhad, I.; Barnes, A. C.; Holbrey, J. D.; Seddon, K. R.; Schwarzacher, W., Templated Electrodeposition of Silver Nanowires in a Nanoporous Polycarbonate Membrane from a Nonaqueous Ionic Liquid Electrolyte. *Appl. Phys. A: Mater. Sci. Process.* **2007**, *86*, 373-375.
2. Hutter, E.; Fendler, J. H., Exploitation of Localized Surface Plasmon Resonance. *Adv. Mater.* **2004**, *16*, 1685-1706.
3. Welch, C. W.; Compton, R. G., The Use of Nanoparticles in Electroanalysis: A Review. *Anal. Bioanal. Chem.* **2006**, *384*, 601-619.

4. Guo, S. J.; Wang, E. K., Synthesis and Electrochemical Applications of Gold Nanoparticles. *Anal. Chim. Acta* **2007**, *598*, 181-192.
5. El-Deab, M. S.; Ohsaka, T., An Extraordinary Electrocatalytic Reduction of Oxygen on Gold Nanoparticles-Electrodeposited Gold Electrodes. *Electrochem. Commun.* **2002**, *4*, 288-292.
6. Murphy, C. J.; Gole, A. M.; Hunyadi, S. E.; Stone, J. W.; Sisco, P. N.; Alkilany, A.; Kinard, B. E.; Hankins, P., Chemical Sensing and Imaging with Metallic Nanorods. *Chem. Commun.* **2008**, 544-557.
7. Jerkiewicz, G.; DeBlois, M.; Radovic-Hrapovic, Z.; Tessier, J. P.; Perreault, F.; Lessard, J., Underpotential Deposition of Hydrogen on Benzene-Modified Pt(111) in Aqueous H<sub>2</sub>SO<sub>4</sub>. *Langmuir* **2005**, *21*, 3511-3520.
8. Hashmi, A. S. K.; Hutchings, G. J., Gold Catalysis. *Angew. Chem. Int. Ed.* **2006**, *45*, 7896-7936.
9. Turner, M.; Golovko, V. B.; Vaughan, O. P. H.; Abdulkin, P.; Berenguer-Murcia, A.; Tikhov, M. S.; Johnson, B. F. G.; Lambert, R. M., Selective Oxidation with Dioxygen by Gold Nanoparticle Catalysts Derived from 55-Atom Clusters. *Nature* **2008**, *454*, 981-983.
10. Lu, Y.; Mei, Y.; Drechsler, M.; Ballauff, M., Thermosensitive Core-Shell Particles as Carriers for Ag Nanoparticles: Modulating the Catalytic Activity by a Phase Transition in Networks. *Angew. Chem. Int. Ed.* **2006**, *45*, 813-816.
11. Sun, Y. G.; Mayers, B.; Xia, Y. N., Transformation of Silver Nanospheres into Nanobelts and Triangular Nanoplates through a Thermal Process. *Nano Letters* **2003**, *3*, 675-679.

12. Ji, X. H.; Song, X. N.; Li, J.; Bai, Y. B.; Yang, W. S.; Peng, X. G., Size Control of Gold Nanocrystals in Citrate Reduction: The Third Role of Citrate. *J. Am. Chem. Soc.* **2007**, *129*, 13939-13948.
13. Chen, D. H.; Wu, S. H., Synthesis of Nickel Nanoparticles in Water-in-Oil Microemulsions. *Chem. Mater.* **2000**, *12*, 1354-1360.
14. Demirci, U. B., Direct Liquid-Feed Fuel Cells: Thermodynamic and Environmental Concerns. *J. Power Sources* **2007**, *169*, 239-246.
15. Gasparotto, L. H. S.; Garcia, A. C.; Gomes, J. F.; Tremiliosi-Filho, G., Electrocatalytic Performance of Environmentally Friendly Synthesized Gold Nanoparticles Towards the Borohydride Electro-Oxidation Reaction. *J. Power Sources* **2012**, *218*, 73-78.
16. Garcia, A.; Gasparotto, L. S.; Gomes, J.; Tremiliosi-Filho, G., Straightforward Synthesis of Carbon-Supported Ag Nanoparticles and Their Application for the Oxygen Reduction Reaction. *Electrocatal.* **2012**, *3*, 147-152.
17. Esumi, K.; Hosoya, T.; Suzuki, A.; Torigoe, K., Formation of Gold and Silver Nanoparticles in Aqueous Solution of Sugar-Persubstituted Poly(Amidoamine) Dendrimers. *J. Colloid Interface Sci.* **2000**, *226*, 346-352.
18. Raveendran, P.; Fu, J.; Wallen, S. L., Completely "Green" Synthesis and Stabilization of Metal Nanoparticles. *J. Am. Chem. Soc.* **2003**, *125*, 13940-13941.
19. Sarkar, A.; Kapoor, S.; Mukherjee, T., Synthesis and Characterisation of Silver Nanoparticles in Viscous Solvents and Its Transfer into Non-Polar Solvents. *Res. Chem. Intermed.* **2010**, *36*, 411-421.

20. Chou, K. S.; Ren, C. Y., Synthesis of Nanosized Silver Particles by Chemical Reduction Method. *Mater. Chem. Phys* **2000**, *64*, 241-246.
21. Halaciuga, I.; LaPlante, S.; Goia, D. V., Precipitation of Dispersed Silver Particles Using Acetone as Reducing Agent. *J. Colloid Interface Sci.* **2011**, *354*, 620-623.
22. Lee, I.-H.; Kwon, H.-K.; An, S.; Kim, D.; Kim, S.; Yu, M. K.; Lee, J.-H.; Lee, T.-S.; Im, S.-H.; Jon, S., Imageable Antigen-Presenting Gold Nanoparticle Vaccines for Effective Cancer Immunotherapy in Vivo. *Angew. Chem. Int. Ed.* **2012**, *51*, 8800-8805.
23. Lima, K. M. G.; Junior, R. F. A.; Araujo, A. A.; Oliveira, A. L. C. S. L.; Gasparotto, L. H. S., Environmentally Compatible Bioconjugated Gold Nanoparticles as Efficient Contrast Agents for Colorectal Cancer Cell Imaging. *Sensor. Actuat. B-Chem.* **2014**, *196*, 306-313.
24. Daniel, M. C.; Astruc, D., Gold Nanoparticles: Assembly, Supramolecular Chemistry, Quantum-Size-Related Properties, and Applications toward Biology, Catalysis, and Nanotechnology. *Chem Rev* **2004**, *104*, 293-346.
25. Moskovits, M.; Srnova-Sloufova, I.; Vlckova, B., Bimetallic Ag-Au Nanoparticles: Extracting Meaningful Optical Constants from the Surface-Plasmon Extinction Spectrum. *J. Chem. Phys.* **2002**, *116*, 10435-10446.
26. Vigneshwaran, N.; Nachane, R. P.; Balasubramanya, R. H.; Varadarajan, P. V., A Novel One-Pot 'Green' Synthesis of Stable Silver Nanoparticles Using Soluble Starch. *Carbohydr. Res.* **2006**, *341*, 2012-2018.

27. Ferreira, E. B.; Gomes, J. F.; Tremiliosi-Filho, G.; Gasparotto, L. H. S., One-Pot Eco-Friendly Synthesis of Gold Nanoparticles by Glycerol in Alkaline Medium: Role of Synthesis Parameters on the Nanoparticles Characteristics. *Materials Research Bulletin* **2014**, *55*, 131-136.
28. Mulvaney, P., Surface Plasmon Spectroscopy of Nanosized Metal Particles. *Langmuir* **1996**, *12*, 788-800.
29. Link, S.; Wang, Z. L.; El-Sayed, M. A., Alloy Formation of Gold–Silver Nanoparticles and the Dependence of the Plasmon Absorption on Their Composition. *J. Phys. Chem. B* **1999**, *103*, 3529-3533.
30. Chou, K.-S.; Lu, Y.-C.; Lee, H.-H., Effect of Alkaline Ion on the Mechanism and Kinetics of Chemical Reduction of Silver. *Mater. Chem. Phys* **2005**, *94*, 429-433.
31. Garcia, A. C.; Lopes, P. P.; Gomes, J. F.; Pires, C. M.; Ferreira, E.; Gasparotto, L. H. d. S.; Tremiliosi-Filho, G.; Lucena, R., Eco-Friendly Synthesis of Bimetallic AuAg Nanoparticles. *New J. Chem.* **2014**, *38*, 2865-2873.
32. Gomes, J. F.; Garcia, A. C.; Pires, C.; Ferreira, E. B.; Albuquerque, R. Q.; Tremiliosi-Filho, G.; Gasparotto, L. H. S., Impact of the AuAg Nps Composition on Their Structure and Properties: A Theoretical and Experimental Investigation. *The Journal of Physical Chemistry C* **2014**, *118*, 28868-28875.
33. Skoog, D. A.; West, D. M.; Holler, F. J., *Fundamentals of Analytical Chemistry*, 7th ed.; Saunders College Publishing: Orlando, 1996, p (apendix 5).
34. Fievet, F.; Lagier, J. P.; Blin, B.; Beaudoin, B.; Figlarz, M., Homogeneous and Heterogeneous Nucleations in the Polyol Process for the Preparation of

Micron and Submicron Size Metal Particles. *Solid State Ionics* **1989**, 32-33, Part 1, 198-205.

35. Lisichkin, A. Y. O. a. G. V., Metal Nanoparticles in Condensed Media: Preparation and the Bulk and Surface Structural Dynamics. *Russ. Chem. Rev.* **2011**, 80, 605-630.

36. Polte, J.; Ahner, T. T.; Delissen, F.; Sokolov, S.; Emmerling, F.; Thünemann, A. F.; Kraehnert, R., Mechanism of Gold Nanoparticle Formation in the Classical Citrate Synthesis Method Derived from Coupled in Situ Xanes and Sxas Evaluation. *J. Am. Chem. Soc.* **2010**, 132, 1296-1301.

37. Selvakannan, P. R.; Swami, A.; Srisathiyarayanan, D.; Shirude, P. S.; Pasricha, R.; Mandale, A. B.; Sastry, M., Synthesis of Aqueous Au Core-Ag Shell Nanoparticles Using Tyrosine as a Ph-Dependent Reducing Agent and Assembling Phase-Transferred Silver Nanoparticles at the Air-Water Interface. *Langmuir* **2004**, 20, 7825-7836.

38. Clayden, J.; Greeves, N.; Warren, S.; Wothers, P., *Organic Chemistry*, first ed.; Oxford University Press: Oxford, 2001, p 283-284.

39. West, A. R., *Solid State Chemistry and Its Applications*; John Wiley & Sons: New York, 1984.

40. Kwon, Y.; Lai, S. C. S.; Rodriguez, P.; Koper, M. T. M., Electrocatalytic Oxidation of Alcohols on Gold in Alkaline Media: Base or Gold Catalysis? *J. Am. Chem. Soc.* **2011**, 133, 6914-6917.

41. Gomes, J.; Tremiliosi-Filho, G., Spectroscopic Studies of the Glycerol Electro-Oxidation on Polycrystalline Au and Pt Surfaces in Acidic and Alkaline Media. *Electrocatal.* **2011**, *2*, 96-105.



## Figure captions

**Figure 1** - UV-vis spectra of the colloidal AuNps produced with the different alkoxide precursors indicated on the picture. Bottom: photographs of the (left) AuNps colloidal dispersion from  $\text{Au}^{3+}$  at alkaline pH and of the (right)  $\text{Au}^{3+}$  solution at neutral or acid pH. Condition of synthesis:  $0.50 \text{ mol L}^{-1}$  alkoxide precursor,  $0.010 \text{ mol L}^{-1}$  NaOH,  $10 \text{ g L}^{-1}$  PVP and  $0.40 \text{ mmol L}^{-1}$   $\text{AuCl}_3$  at  $25 \text{ }^\circ\text{C}$ .

**Figure 2** - TEM images of the colloidal AuNps produced with the different alkoxide precursors indicated on the picture. Condition of synthesis:  $0.50 \text{ mol L}^{-1}$  alkoxide precursor,  $0.010 \text{ mol L}^{-1}$  NaOH,  $10 \text{ g L}^{-1}$  PVP and  $0.40 \text{ mmol L}^{-1}$   $\text{AuCl}_3$  at  $25 \text{ }^\circ\text{C}$ .

**Figure 3** - UV-vis spectra of the colloidal AgNps produced with the different alkoxide precursors indicated on the picture. Bottom: photographs of the (left) AgNps colloidal dispersion from  $\text{Ag}^+$  at alkaline pH and of the (right)  $\text{Ag}^+$  solution at neutral or acid pH (right). Condition of synthesis:  $0.50 \text{ mol L}^{-1}$  alkoxide precursor,  $0.010 \text{ mol L}^{-1}$  NaOH,  $10 \text{ g L}^{-1}$  PVP and  $0.40 \text{ mmol L}^{-1}$   $\text{AgNO}_3$  at  $25 \text{ }^\circ\text{C}$ .

**Figure 4** - TEM images of the colloidal AgNps produced with the different alkoxide precursors indicated on the picture. Condition of synthesis:  $0.50 \text{ mol L}^{-1}$  alkoxide precursor,  $0.010 \text{ mol L}^{-1}$  NaOH,  $10 \text{ g L}^{-1}$  PVP and  $0.40 \text{ mmol L}^{-1}$   $\text{AgNO}_3$  at  $25 \text{ }^\circ\text{C}$ .

**Figure 5** – (A) UV-vis spectra and (B) TEM images of bimetallic AuAg-Nps produced at  $\text{Au}^{3+}/\text{Ag}^+$  molar ratio of 0.5 at different pH values (indicated on the picture). Other parameters:  $0.50 \text{ mol L}^{-1}$  glycerol,  $10 \text{ g L}^{-1}$  PVP,  $0.20 \text{ mmol L}^{-1}$   $\text{AuCl}_3$  and  $0.20 \text{ mmol L}^{-1}$   $\text{AgNO}_3$  at  $25 \text{ }^\circ\text{C}$ .

**Figure 6** – UV-vis spectra and TEM images of Au-Nps and Ag-Nps synthesized by  $0.10 \text{ mol L}^{-1}$  potassium tert-butoxide under neutral conditions. Other parameters:  $10 \text{ g L}^{-1}$  PVP,  $0.40 \text{ mmol L}^{-1}$   $\text{AuCl}_3$  and  $0.40 \text{ mmol L}^{-1}$   $\text{AgNO}_3$  at  $25 \text{ }^\circ\text{C}$ .

**Figure 7** – HPLC results of  $0.010 \text{ mol L}^{-1}$  glycerol in  $0.010 \text{ mol L}^{-1}$  NaOH and Ag nanoparticles synthesis samples taken at 1 min, 30 min and 60 min. Condition of synthesis:  $0.010 \text{ mol L}^{-1}$  glycerol,  $0.010 \text{ mol L}^{-1}$  NaOH and  $0.4 \text{ mmol L}^{-1}$   $\text{AgNO}_3$  at  $25 \text{ }^\circ\text{C}$ .

**Figure 8** – HPLC results of  $0.010 \text{ mol L}^{-1}$  glycerol in  $0.010 \text{ mol L}^{-1}$  NaOH and Au nanoparticles synthesis samples taken at 1 min, 30 min and 60 min. Condition of synthesis:  $0.010 \text{ mol L}^{-1}$  glycerol,  $0.010 \text{ mol L}^{-1}$  NaOH and  $0.4 \text{ mmol L}^{-1}$   $\text{AgNO}_3$  at  $25 \text{ }^\circ\text{C}$ . Peaks labeled A, B, C, E, F, G and H are associated with the possible formation of oxalic acid, tartronic acid, hydroxypyruvic acid, glyceric acid and/or glyceraldehyde, glycolic acid, dihydroxyacetone and formic acid, respectively. Peak D was not identified to be related with any of the reference samples investigated here.

**Figure 9** – (Top) TEM images of the Au/C, Au<sub>50</sub>Ag<sub>50</sub>/C and Ag/C catalysts. (Bottom) Polarization curves for borohydride and glycerol eletro-oxidations over Au/C, glycerol electro-oxidation over Au<sub>50</sub>Ag<sub>50</sub>/C and oxygen electroreduction over Ag/C in alkaline medium. For borohydride oxidation: 1.0 mmol L<sup>-1</sup> NaBH<sub>4</sub><sup>-</sup> + 1.0 mol L<sup>-1</sup> NaOH; 1600 rpm;  $\nu = 5.0 \text{ mV s}^{-1}$ . For glycerol oxidation: 0.10 mol L<sup>-1</sup> glycerol + 0.10 mol L<sup>-1</sup> NaOH;  $\nu = 50 \text{ mV s}^{-1}$ . For oxygen reduction: O<sub>2</sub>-saturated 1.0 mol L<sup>-1</sup> NaOH; 1600 rpm;  $\nu = 5.0 \text{ mV s}^{-1}$ .

Figure 1

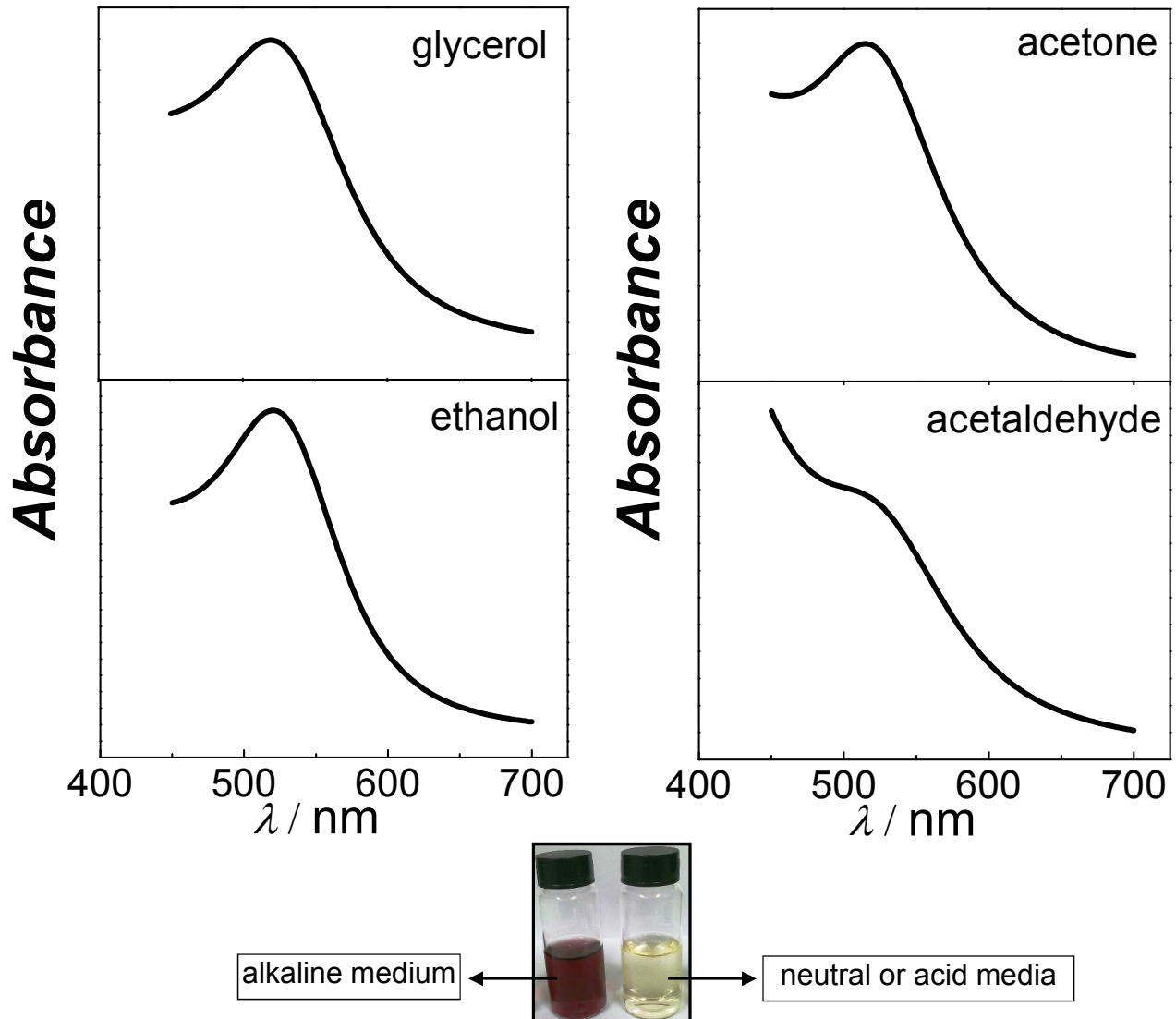


Figure 2

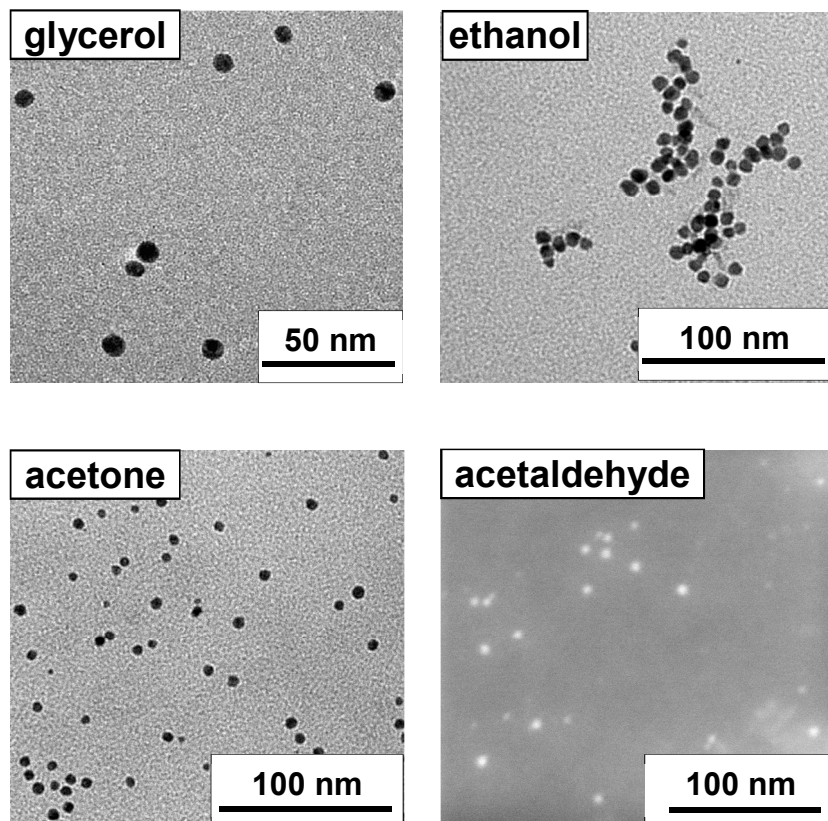


Table 1  
Average sizes of Au-Nps and Ag-Nps obtained with different alkoxide precursors

precursor	Au-Nps size (nm)	Ag-Nps size (nm)
glycerol	7.6 ( $\pm$ 1.4)	20.1 ( $\pm$ 4.6)
ethanol	6.8 ( $\pm$ 1.1)	-
acetone	4.6 ( $\pm$ 1.3)	10.7 ( $\pm$ 2.7)
acetaldehyde	4.6 ( $\pm$ 1.3)	36.1 ( $\pm$ 1.7)
methanol	-	11.2 ( $\pm$ 2.6)

Figure 3

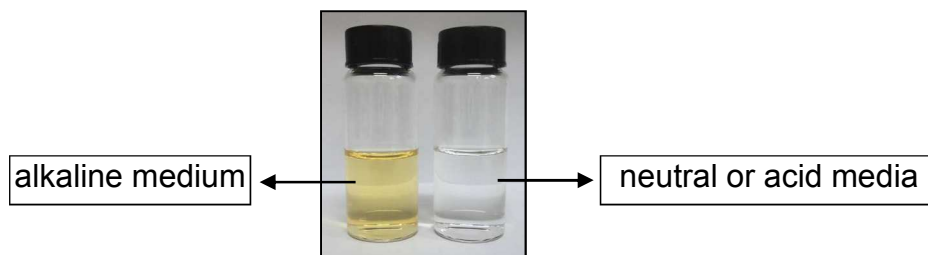
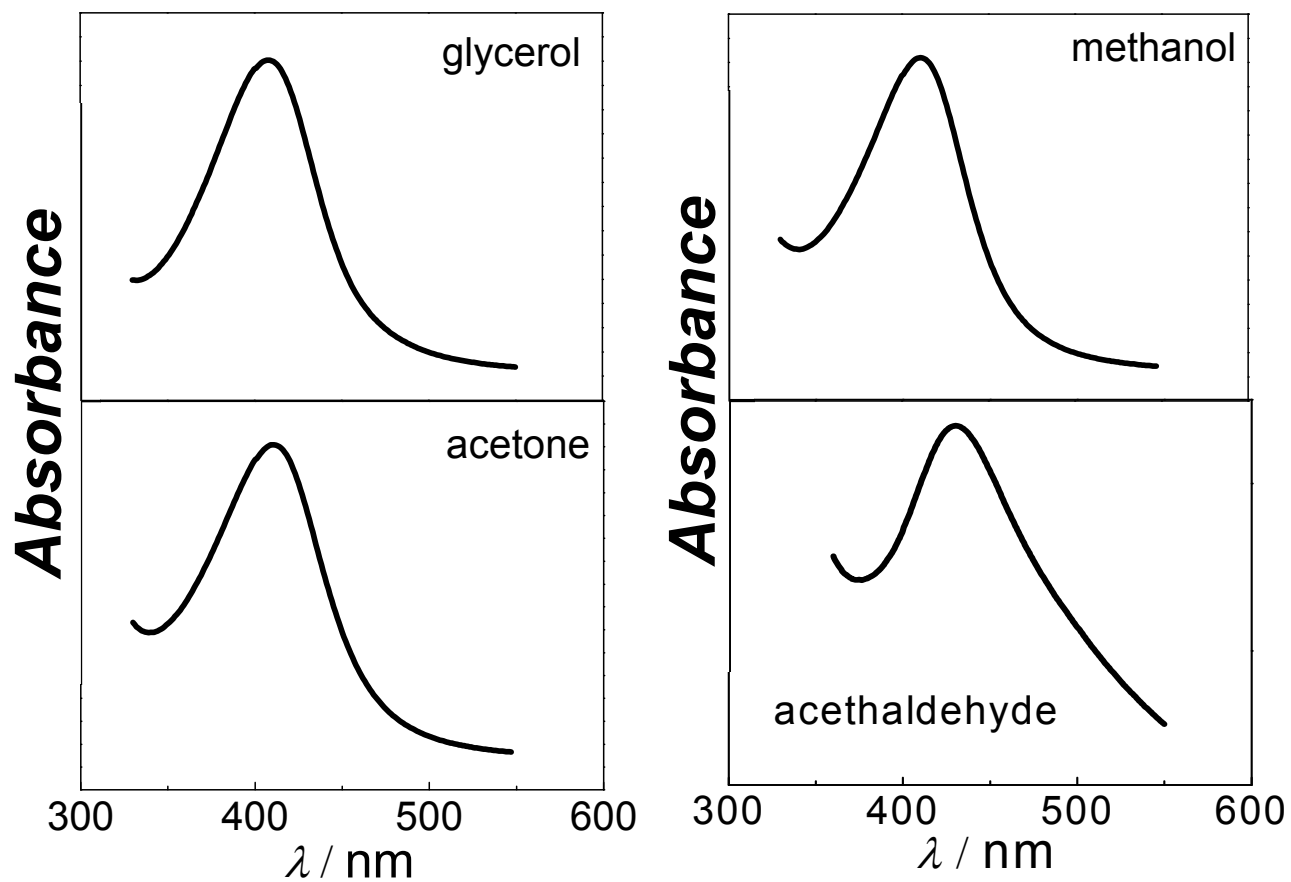


Figure 4

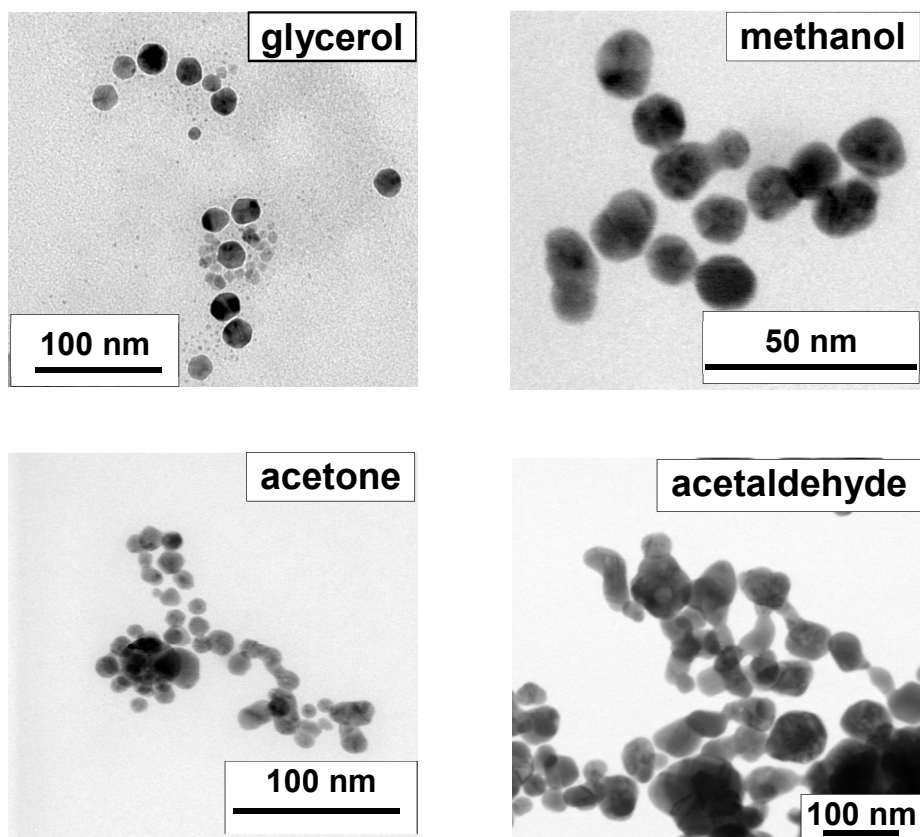


Figure 5

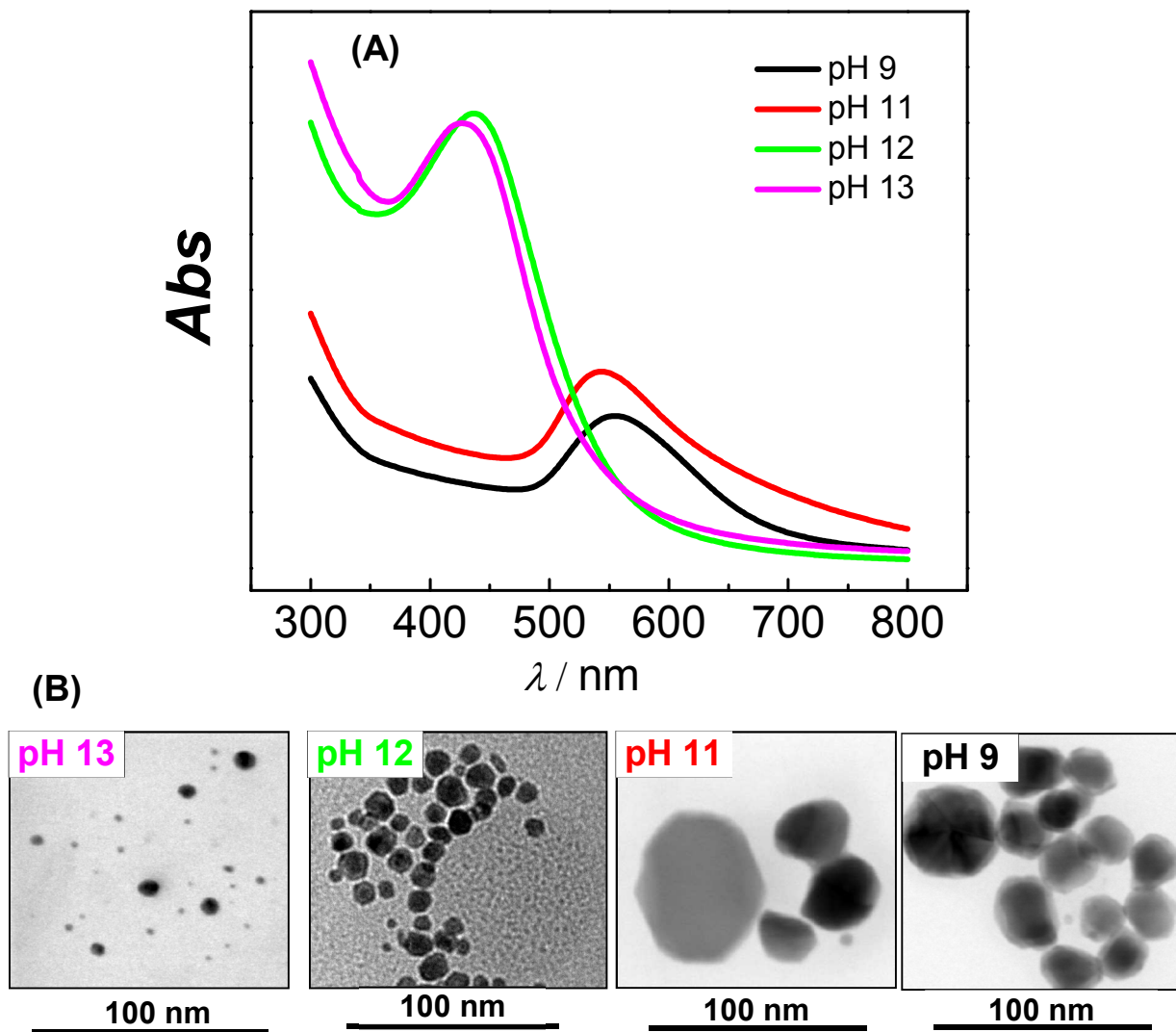


Table 2 – Composition of AuAg-Nps as a function of pH

pH	Composition (Au %)
9.0	98
11	92
12	61
13	56



Figure 6

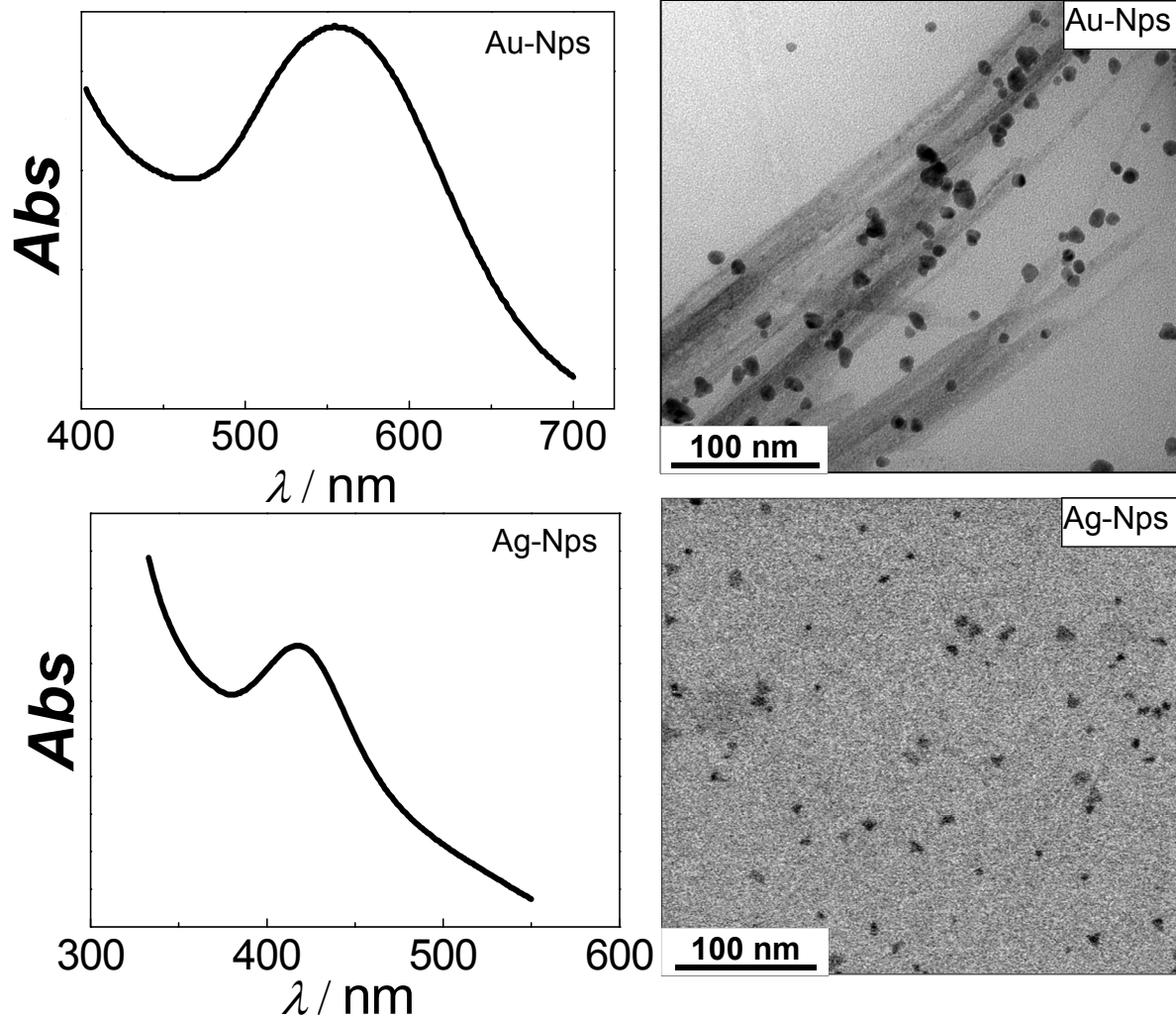


Figure 7

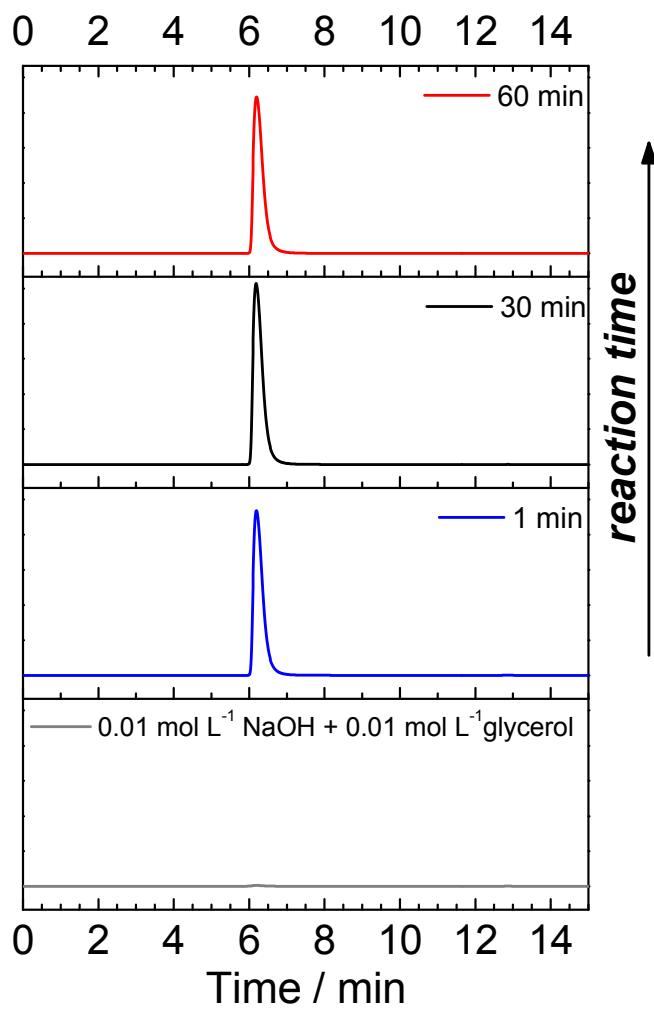


Figure 8

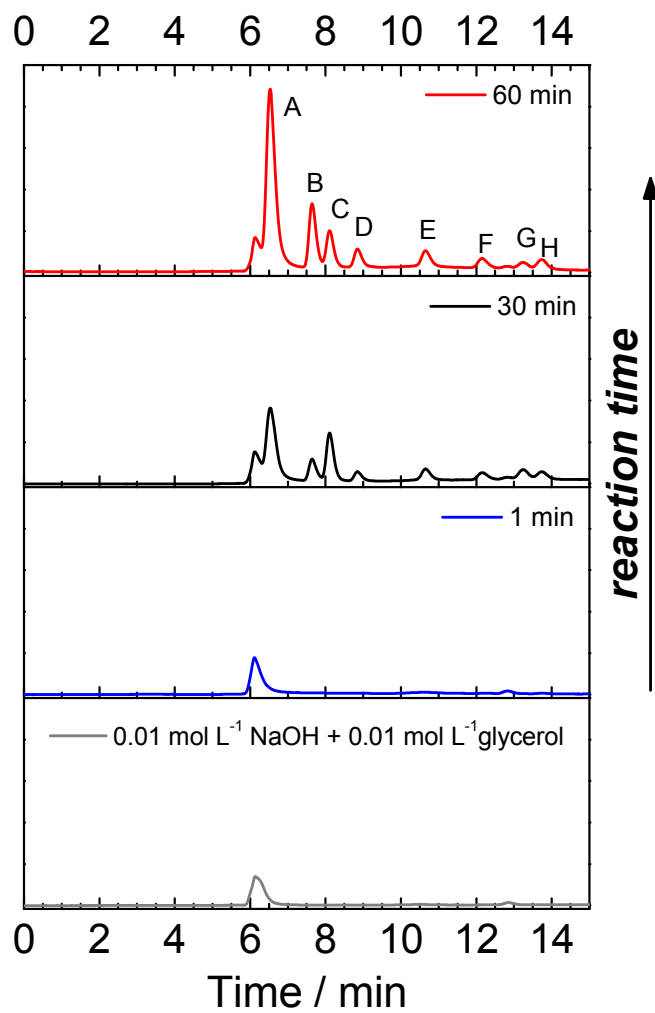
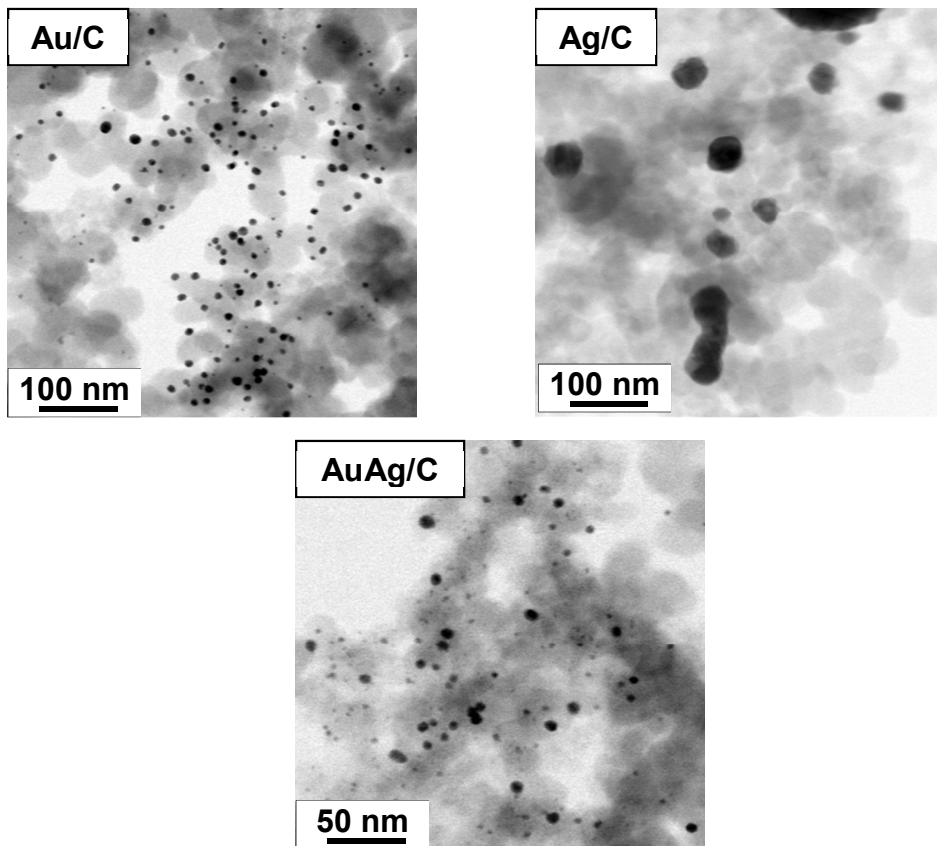


Figure 9

(A)



(B)

